

*Electronic supplementary information for*

# Mechanistic Insights into the Halogenated Solvent Effect on the Au-S Bond Cleavage

*Sha Yang<sup>\*a‡</sup>, Yirong Zhang<sup>a‡</sup>, Wei Liu<sup>\*b</sup>*

<sup>a</sup>Nano and Heterogeneous Materials Center, School of Materials Science and Engineering,  
Nanjing University of Science and Technology, Nanjing 210094, Jiangsu, China.

<sup>b</sup>State Key Laboratory of Rare Earth Resource Utilization, Changchun Institute of Applied  
Chemistry, Chinese Academy of Sciences, Changchun 130022, China.

## Computational methods

All DFT calculations were carried out by using the Vienna Ab initio Simulation Package (VASP).<sup>1</sup> Structural optimizations and energy calculations were performed using the Grimme van der Waals (vdW) correction method,<sup>2</sup> coupled to Perdew-Burke-Ernzerhof (PBE) functional.<sup>3</sup> The energy convergence criterion was set to  $10^{-5}$  eV, and the structures were optimized until the forces on each atom fell below 0.05 eV/Å. A  $3 \times 3 \times 1$  Monkhorst-Pack k-point mesh was used for the Brillouin zone sampling.<sup>4</sup> A periodic four-layer Au tetrahedron was used to construct the electrode, with the bottommost layer fixed. To avoid periodic interactions, the junctions were put into a cell with size of  $18 \times 18 \times 35$  Å.

The climbing-image nudged elastic band (CI-NEB) method<sup>5</sup> was employed to determine the dissociation barriers of halogenated solvents on the gold electrode, with five images inserted to search the transition states. Crystal orbital Hamiltonian population (COHP) calculations were performed using the LOBSTER package<sup>6-8</sup> to analyze the interfacial bonding and anti-bonding states. To investigate the dynamic behavior of Au-S contacts in BDSAc and BDT molecular junctions, ab initio molecular dynamics (AIMD) calculations were performed in the canonical NVT ensemble for 5 ps with a time step of 2 fs, at temperatures of 300, 600, and 800 K. During AIMD simulations, the two bottommost layers of each tetrahedron electrode and the halogen atoms in solvent molecules were fixed, while the remaining atoms were fully relaxed. Molecular conductance was calculated by the non-equilibrium Green's function (NEGF) method in the framework of DFT, implemented in Atomistix ToolKit (ATK).<sup>9</sup> The exchange-correlation functional is treated by the PBE formulation, together with FHI pseudopotentials with double- $\zeta$ -polarized (DZP) basis set. Although the calculated conductance is overestimated due to the electron self-interaction error inherent in the PBE functional<sup>10</sup>, this limitation does not qualitatively affect our conclusions. The Brillouin zone was sampled using a  $4 \times 4 \times 150$  Monkhorst-Pack grid for the two electrodes.

To assess the solvent effect on junction contact stability, we calculated the binding energy between the target molecule and the electrode. For solvent-free junctions, the binding energy was defined as the total energy of the junction minus the energies of the isolated target molecule and the pristine electrode. In the presence of solvent, the binding energy was approximated by subtracting three terms from the total junction energy: the energy of the solvent-adsorbed electrode, the energy of the free target molecule, and the molecule-solvent interaction energy. The

latter term was calculated as the total energy of the molecule-solvent complex minus the sum of their individual energies, each fixed at the geometry they adopt within the relaxed junction structure.

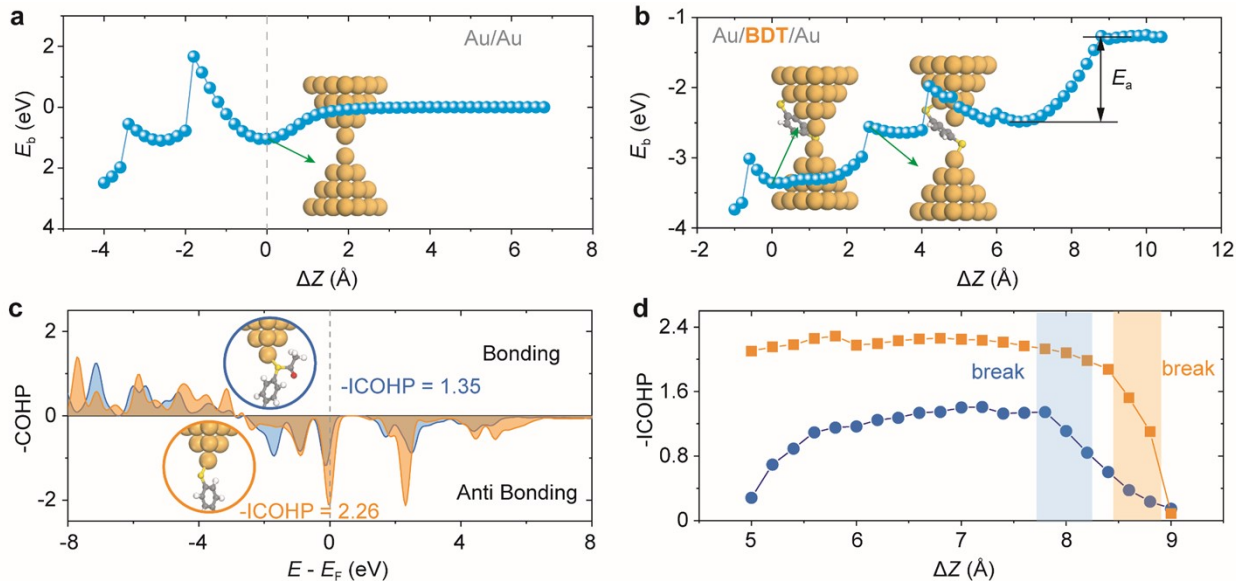


**Fig. S1** Energy profile during the formation of Au/Au (a) and Au/BDT/Au junctions (b) as a function of electrode distance. The zero distance corresponds to formation of a single Au-Au bond, denoted by the insets. (c) COHP analysis for the upper Au-S bond in Au/BDSAc/Au (blue) and Au/BDT/Au (orange) junctions at an electrode distance of 6.8 Å. The values represent the corresponding  $-\text{ICOHP}$  at the Fermi level. (d) Values of  $-\text{ICOHP}$  for the upper Au-S bond in Au/BDSAc/Au (blue) and Au/BDT/Au (orange) junctions as a function of electrode distance. The blue and orange regions denote the possible rupture distances.

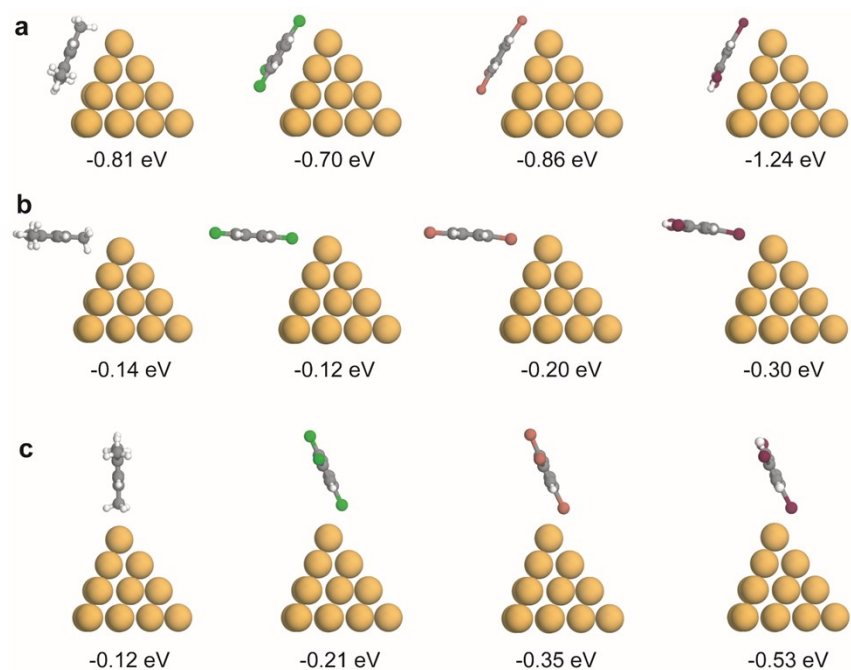


**Fig. S2** Adsorption structures and energies of TMB, TCB, TBB, and TIB solvents on electrodes with various configurations. Given the asymmetric structures of TCB and TBB solvents used in this work, adsorption configurations with the chlorine or bromine atoms at the 1- or 2-position facing the electrode terminals have also been considered. The calculated adsorption energies for these configurations are  $-0.66$  eV for TCB and  $-0.78$  eV for TBB, which are slightly higher than that of the structures in (a). The adsorption energies in (b) and (c) primarily reflect the binding strength between the electrode terminals and the methyl groups (in TMB) or halogen atoms (in halogenated solvents).

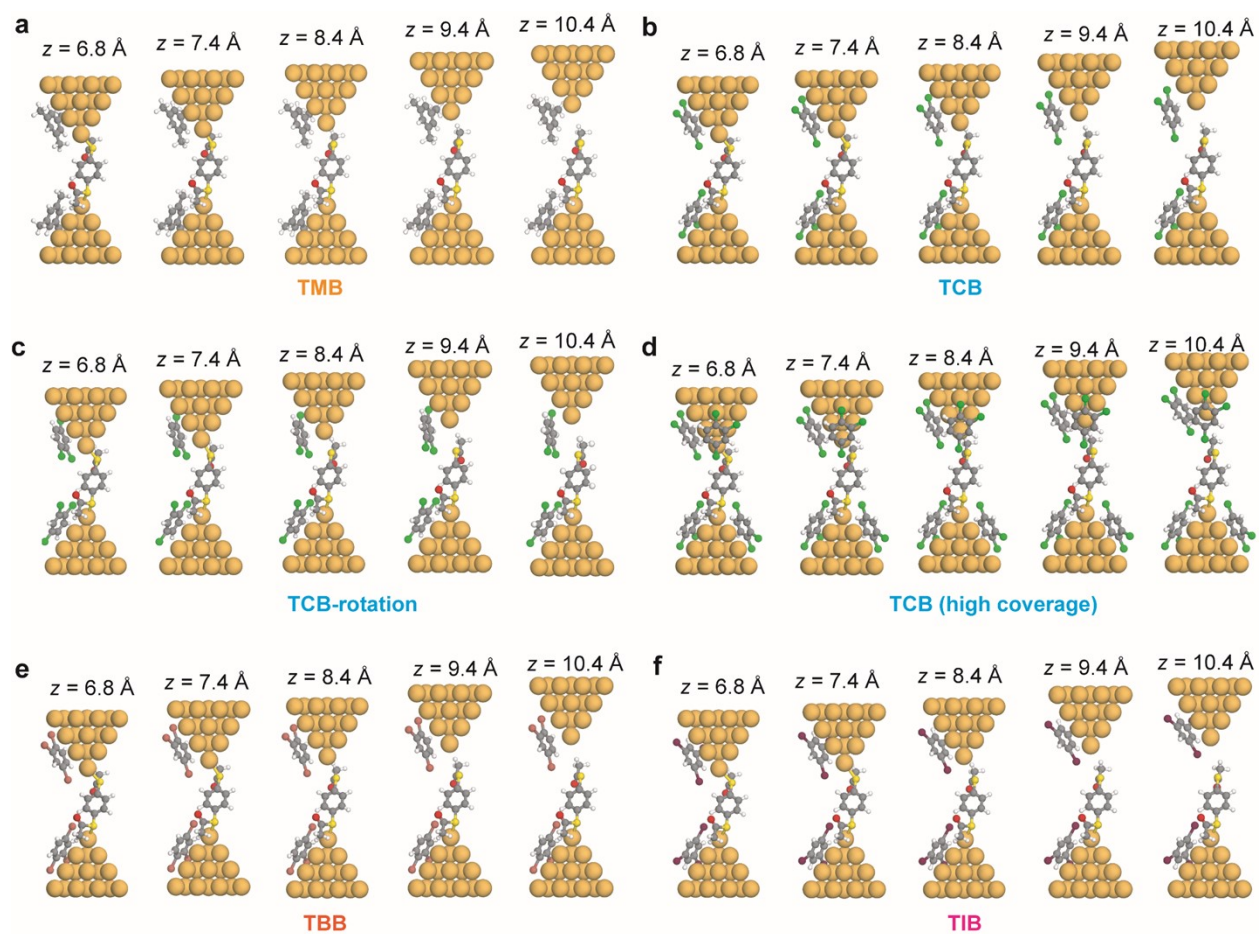


**Fig. S3** Structure evolutions during formation of Au/BDSAc/Au junction under TMB (a), TCB (b)-(d), TBB (e), TIB (f) solutions.

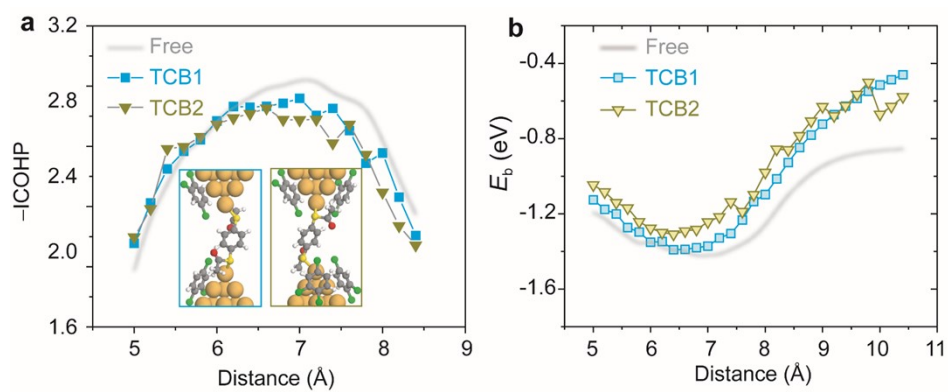


**Fig. S4** Values of  $-\text{ICOHP}$  for Au-S bonds (a) and molecule-electrode binding energies (b) in Au/BDSAc/Au junctions under free (gray), low-coverage TCB (blue), and high-coverage TCB (dark green) conditions.

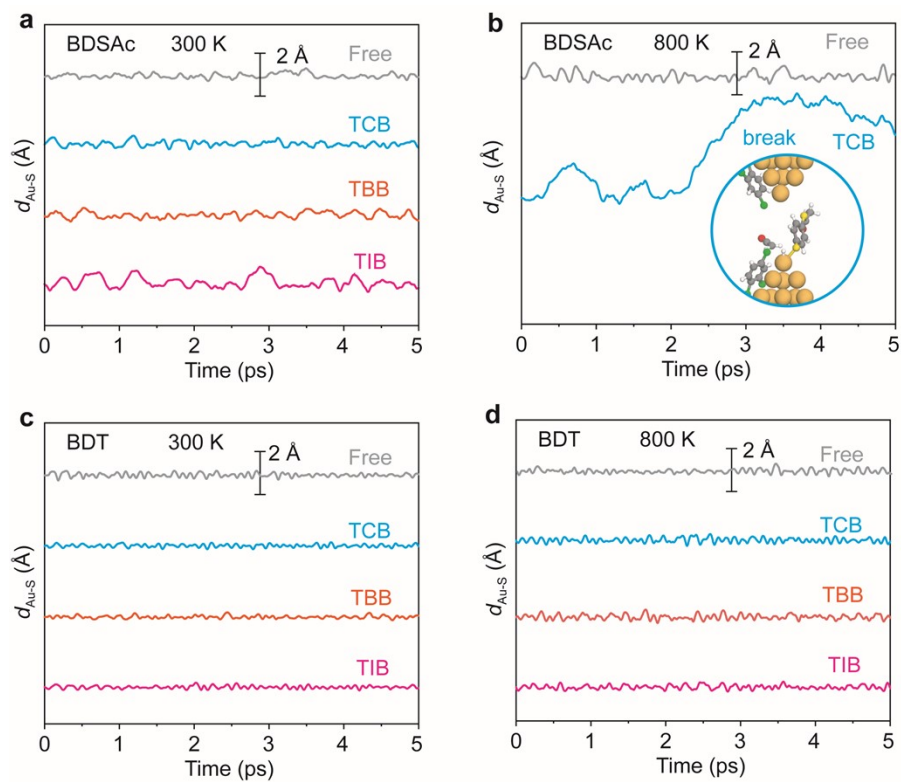


**Fig. S5** Evolution of Au-S bond length for BDSAc (a-b) and BDT (c-d) junction under various solvent condition through 5-ps AIMD simulations at 300 and 800 K.



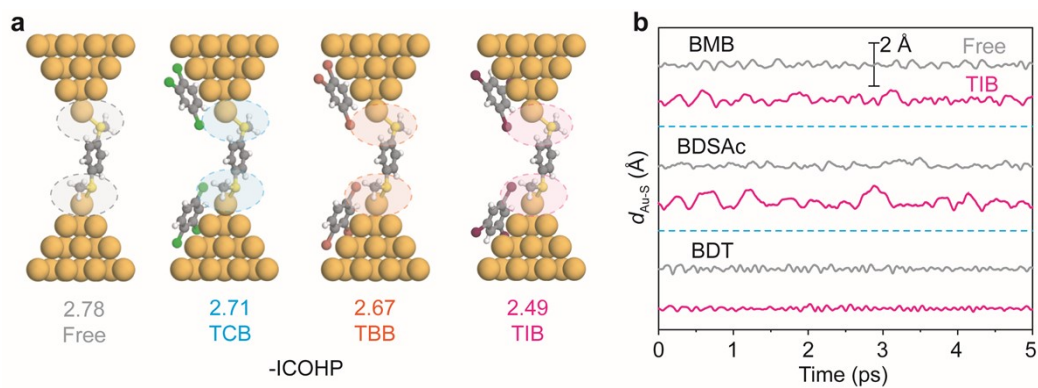


**Fig. S6** (a) Structures of BMB junctions and the corresponding -ICOHP values for the Au-S bonds under various solvent conditions at an electrode displacement of 6.6 Å. (b) Evolution of Au-S bond length for BMB, BDSAc, and BDT junctions in 5-ps AIMD simulations at 300 K.

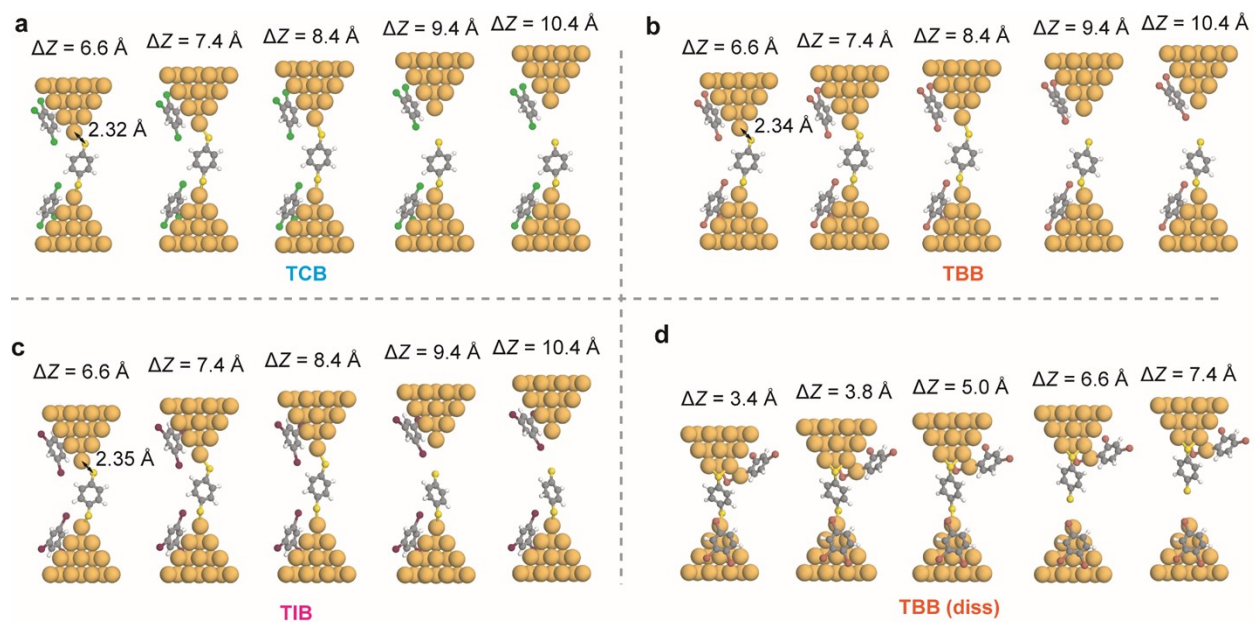


**Fig. S7** Structure evolutions during formation of Au/BDT/Au junctions under TCB (a), TBB (b), TIB (c), and dehalogenated TBB conditions.

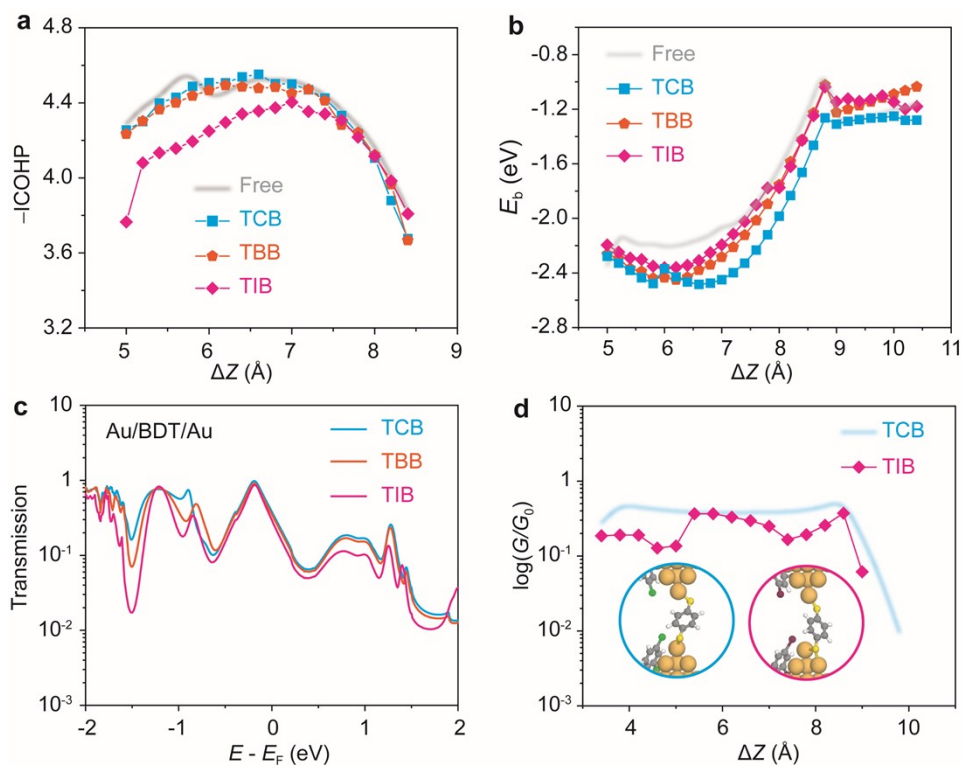


**Fig. S8** Values of  $-ICOHP$  for Au-S bonds (a) and molecule-electrode binding energies (b) in Au/BDT/Au junctions under solvent-free (gray), TCB (blue), TBB (red), and TIB (pink) conditions. (c) Transmission spectra for BDT junctions in TCB, TBB, and TIB solvents with electrode displacement of 6.6 Å. (d) Molecular conductance trace for BDT junction in TIB solvents.

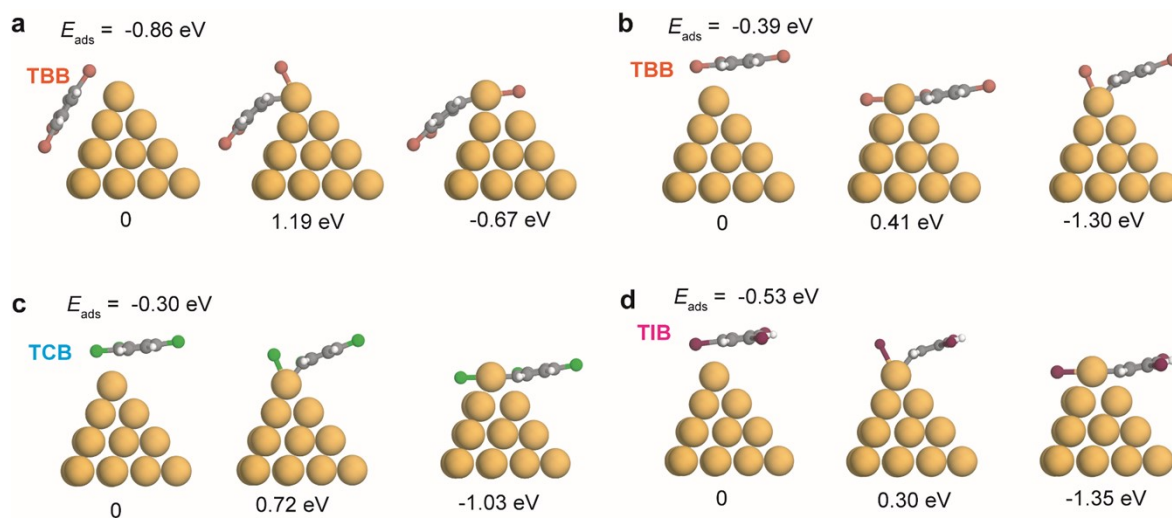


**Fig. S9** Dehalogenation reaction pathways for TBB, TCB, and TIB molecules on electrodes. Structures and Gibbs energies of initial state (IS), transition state (TS), and final state (FS) of TBB (a-b), TCB (c), and TIB (d) on gold electrodes.

## References

- (1) Kresse, G.; Furthmüller, J. Efficient iterative schemes for *ab initio* total-energy calculations using a plane-wave basis set. *Physical Review B* **1996**, *54* (16), 11169.
- (2) Grimme, S.; Ehrlich, S.; Goerigk, L. Effect of the damping function in dispersion corrected density functional theory. *Journal of Computational Chemistry* **2011**, *32* (7), 1456-1465.
- (3) Perdew, J. P.; Burke, K.; Ernzerhof, M. Generalized Gradient Approximation Made Simple. *Physical Review Letters* **1996**, *77* (18), 3865-3868.
- (4) Monkhorst, H. J.; Pack, J. D. Special points for Brillouin-zone integrations. *Physical Review B* **1976**, *13*, 5188-5192.
- (5) Henkelman, G.; Uberuaga, B. P.; Jonsson, H. A climbing image nudged elastic band method for finding saddle points and minimum energy paths. *Journal of Chemical Physics* **2000**, *113* (22), 9901-9904.
- (6) Dronskowski, R.; Bloechl, P. E. Crystal orbital Hamilton populations (COHP): energy-resolved visualization of chemical bonding in solids based on density-functional calculations. *The Journal of Physical Chemistry* **1993**, *97* (33), 8617-8624.
- (7) Deringer, V. L.; Tchougréeff, A. L.; Dronskowski, R. Crystal Orbital Hamilton Population (COHP) Analysis As Projected from Plane-Wave Basis Sets. *The Journal of Physical Chemistry A* **2011**, *115* (21), 5461-5466.
- (8) Maintz, S.; Deringer, V. L.; Tchougréeff, A. L.; Dronskowski, R. LOBSTER: A tool to extract chemical bonding from plane-wave based DFT. *Journal of Computational Chemistry* **2016**, *37* (11), 1030-1035.
- (9) ATOMISTIX TOOLKIT, version 2018.06, QuantumWise A/S.
- (10) Souza, A. d. M.; Rungger, I.; Pontes, R. B.; Rocha, A. R.; da Silva, A. J. R.; Schwingenschlöegl, U.; Sanvito, S. Stretching of BDT-gold molecular junctions: thiol or thiolate termination? *Nanoscale* **2014**, *6* (23), 14495-14507.